Available online at www.sciencedirect.com
ScienceDirect
International Journal of Multiphase Flow 33 (2007) 1308–1319
International Journal of Multiphase Flow
www.elsevier.com/locate/ijmulflow

The transient buoyancy driven motion of bubbles across a two-dimensional quiescent domain

Souvik Biswas, Gretar Tryggvason *

Worcester Polytechnic Institute, Worcester, MA 01609, United States

Received 15 January 2007; received in revised form 19 June 2007

Abstract

The transient buoyancy driven motion of two-dimensional bubbles across a domain bounded by two horizontal walls is studied by direct numerical simulations. The bubbles are initially released next to the lower wall and as they rise, they disperse. Eventually all the bubbles collect at the top wall. The goal of the study is to examine how a simple one-dimensional model for the averaged void fraction captures the unsteady bubble motion. By using void fraction dependent velocities, where the exact dependency is obtained from simulations of homogeneous bubbly flows, the overall dispersion of the bubbles is predicted. Significant differences remain, however. We suggest that bubble dispersion by the bubble induced liquid velocity must be included, and by using a simple model for the bubble dispersion we show improved agreement.

Keywords: Bubbly flows; Direct numerical simulations; Two-fluid model

1. Introduction

Multiphase flows in general and bubbly flows in particular are extremely common, both in nature and in industrial processes. Example of bubbly multiphase flows include the formation of bubbles from dissolved gasses in volcanic eruptions, air entrainment near the ocean surface, vapor bubbles in boiling, and bubbles used to stir metal melts. Although the properties of the bubble/liquid mixture is often determined by what happens at the bubble scale, many bubble systems are very large and it is the averaged or bulk properties of the mixture that are of most practical interest. Several model equations have been proposed to predict the average motion, ranging from simple mixture models, treating the mixture as one fluid, to more sophisticated two-fluid models where each phase is treated separately. In all cases, information about the small-scale behavior is lost in the averaging and closure terms must be introduced to describe the influence of the (unresolved) small-scales on the resolved large-scale motion. The key to modeling the average behavior of two-phase flows is the existence of universal closure relations between macroscopic quantities. Thus, just as transport coefficients for

* Corresponding author.
E-mail address: gretar@wpi.edu (G. Tryggvason).

0301-9322/$ - see front matter © 2007 Elsevier Ltd. All rights reserved.
doi:10.1016/j.ijmultiphaseflow.2007.06.006

constitutive laws in continuum theories apply everywhere, it should ideally be possible to use phenomenological coefficients developed for one situation to predict what will happen in a different situation. While two-phase flow certainly exhibit considerable amount of universality at the smallest scales (otherwise any attempts to develop closure relations for the average motion would be hopeless), the absence of a clear separation of scales makes closure a much more challenging task than is usually the case for continuum theories.

Two-fluid models for multiphase flows were introduced by Spalting (1980) and Harlow and Amsden (1975). For detailed derivations and discussions of the various version of the two-fluid model, see Delhaye and Boure (1982), Kataoka and Serizawa (1989), Zhang and Prosperetti (1994), Drew and Passman (1998), and Prosperetti and Tryggvason (2007). Applications of two-fluid models to bubbly flows in pipes can be found in Antal et al. (1991), De Bertodano et al. (1987, 1994), Kuo et al. (1997), Azpitarte and Buscaglia (2003), Politano et al. (2003) and Celik and Gel (2002), Guet et al. (2005), and Biswas et al. (2005) for example.

For bubbly flows, direct numerical simulations or DNS – where every continuum length and time scale is fully resolved for the unsteady motion of a system containing a range of scales – have recently lead to a very detailed information for homogeneous bubbly flows at low and modest Reynolds numbers, see Esmaeeli and Tryggvason (1998, 1999, 2005) and Bunner and Tryggvason (2002, 2003). Similar computations for more complex flows, such as bubbly flows in vertical channels (Lu et al., 2006), are also starting to emerge.

In this paper, we examine a very simple model problem where a cloud of buoyant bubbles moves across a horizontal channel. To model the evolution of the void fraction profile we use data obtained by simulations of homogeneous bubbly flows to provide a relation for the dependency of the bubble slip velocity on the void fraction. The key questions are how well the model, derived using small bubbles and a dilute flow, performs in situations that are easily simulated (large bubbles and dense flow), and how many ensembles needs to be simulated to get a well converged average flow behavior. To allow us to easily compute several cases (with slightly different initial conditions) for a relatively large system, we assume that the motion is two-dimensional.

2. Problem setup and modeling

We examine the transient migration of bubbles in a horizontal channel, with gravity acting downward, normal to the top and bottom walls. See Fig. 1, where we define the vertical coordinate as y and x as the horizontal coordinate. The bubbles rise upwards due to gravity. There is no pressure gradient in either the x or the y-direction and the liquid is initially at rest. The flow is assumed to be homogeneous on the average in the x-direction ($\partial/\partial x = 0$). Here, we limit our considerations to systems with bubbles of only one size, so the rise of the bubbles is determined by the Archimedes number, N, and the Eötvös number, Eo. In addition, we need

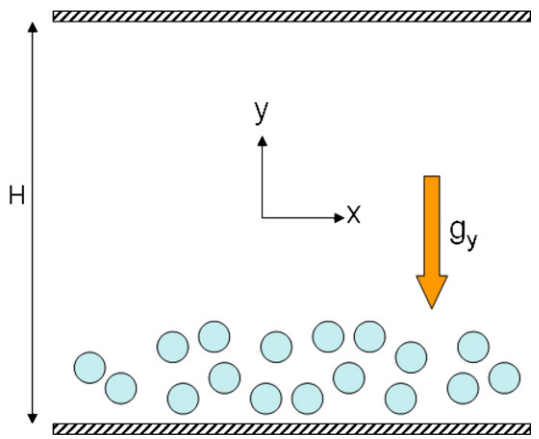

Fig. 1. The problem setup. The horizontal channel is bounded by walls in the y-direction and is periodic in the x-direction. The height of the channel is H and gravity acts in the negative y-direction. The bubbles are released from near the bottom of the channel and rises upwards until they hit the top wall.

to specify either the distribution of the bubbles or the void fraction distribution, α, as function of the vertical distance, as well as the size of the domain. The governing non-dimensional numbers, therefore, are

$$Eo = \frac{\rho_l d_b^2 g}{\sigma}; \quad M = \frac{g\mu_l^4}{\rho_l \sigma^3}; \quad \alpha(y^*); \quad \frac{H}{d_b}.$$

Here H is the height of the channel, ρ_l and μ_l are the liquid density and viscosity, respectively, σ is the surface tension, g is the gravity acceleration, and d_b is diameter of the (un-deformed) bubbles. When presenting the results, length is non-dimensionalized by the bubble diameter d_b, time by $\tau = \left(\sqrt{d_b/g}\right)$, kinetic energy by $u^{*2} = (d_b g)$ and velocities are given as Reynolds numbers $Re = \rho_l V d_b/\mu_l$.

The motion of the bubbles is computed by solving the full Navier–Stokes equations in the whole domain, both in the liquid and inside the bubbles. Using a front-tracking/finite-volume method, we solve the governing equations on a fixed, regular mesh, explicitly tracking the bubble surface by connected marker points (Unverdi and Tryggvason, 1992; Tryggvason et al., 2001). The method has been used earlier for a large number of simulations of bubbly multiphase flows and both the code and various validation tests have been described in detail in several publications, see Esmaeeli and Tryggvason (1999), for example.

The two-fluid model for multiphase flow is based on writing separate conservation equations for mass and momentum for each phase. In the problem we study here, where there is no net flow, the model simplifies considerably. We do not, in particular, need to consider the momentum equation in the liquid, since the liquid flow is determined completely by the bubble slip velocity. The conservation equation for the void fraction, $\alpha = \alpha_g = 1 - \alpha_l$, is given by

$$\frac{\partial \alpha}{\partial t} + \frac{\partial}{\partial y}(\alpha v_g) = 0, \tag{1}$$

where v_g is the gas velocity in the y-direction. For the liquid we replace α_g by α_l and v_g by v_l (the liquid velocity). Adding the conservation equation for the gas and the liquid, we get

$$\frac{\partial}{\partial y}\left[\alpha v_g + (1-\alpha)v_l\right] = 0. \tag{2}$$

Using the boundary conditions that the velocity in y-direction at the top and bottom walls is zero for both phases, we find that

$$\alpha v_g + (1-\alpha)v_l = 0. \tag{3}$$

The average bubble slip velocity in the y-direction is $v_s(=v_g - v_l)$, so

$$v_g = (1-\alpha)v_s, \quad v_l = -\alpha v_s. \tag{4}$$

In general the motion of the bubbles is unsteady and even when the bubbles achieve their steady-state slip velocity, there is a short transient before they do so. This transient is, however, often short and here we will assume that on the average the bubble slip velocity can be taken to depend only on the local void fraction (α). Thus, any dependency on the void fraction gradient is ignored as well as any transient adjustment period associated with a change in the local void fraction. Thus, if v_s is known as a function of α, we can find the void fraction as a function of time by solving Eq. (1), using (4).

3. Results

The goal here is to investigate how realistic it is to use data from DNS of relatively simple systems to model the evolution of more complex flows. To find the unsteady evolution of the average void fraction for the situation sketched in Fig. 1, using Eq. (1), we need the bubble slip velocity as a function of the void fraction and we want to use data from simulations of homogeneous flows to generate that data. In doing so we make two assumptions: First of all we assume that the bubble velocity depends on the void fraction in the same way it does in homogeneous flows and, in particular, that the velocity depends only on the void fraction and not the gradient of the void fraction. Second, we assume that any transient phase of the bubble motion is sufficiently short, compared to the characteristic bubble rise time, so that the instantaneous bubble velocity is well

approximated by the steady-state velocity at the corresponding local void fraction. Although Esmaeeli and Tryggvason (1999) have reported data for the void fraction dependency of the average slip velocity for homogeneous two-dimensional bubbly flow, the governing parameters selected here are slightly different so we regenerated the data for exactly our situation by following the motion of 25 bubbles in fully periodic domains until they had reached a statistically steady state, for several values of α. We took $Eo = 0.2813$ and $M = 4.88 \times 10^{-8}$ and the void fraction was varied by changing the size of the domain. Fig. 2 shows the average slip velocity of the bubbles versus the void fraction obtained in this way, along with the bubble distribution at one time, for one void fraction. We note that we have not examined the rise velocity for a different number of bubbles. The emergence of an inverse energy cascade in two-dimensional flows can lead to domain size dependent rise velocity (Esmaeeli and Tryggvason, 1996), but as Esmaeeli and Tryggvason (1999) showed, the effect is generally reduced as the Reynolds number increases.

Having obtained the bubble slip velocity as a function of the void fraction for homogeneous flows, we proceed to examine how this relation applies to a more complex situation. To study the system sketched in Fig. 1, we follow the motion of 81 bubbles as they rise in an initially quiescent liquid. The diameter of the initially circular bubbles is 0.03 times the height of the domain and Eo and M are the same as used for the data shown in Fig. 2. The width of the domain is equal to its height and we impose periodic boundary conditions in the horizontal direction. The domain is resolved by a 769 by 768 grid. For computational convenience we take the bubble density and viscosity to be one-tenth of the liquid. As discussed by Esmaeeli and Tryggvason (1999), reducing the density and viscosity of the bubbles has essentially no impact on the results. Fig. 3 shows the bubble distribution and the stream lines at different times for one particular simulation. The velocity is initially zero everywhere and the bubbles are located near the bottom wall at the start of the simulation (frame a). The vertical location of the bubbles is determined using a Gaussian distribution of random numbers, but the horizontal location is set "by hand" to ensure that the bubbles do not overlap. As they rise, their motion induces a non-zero velocity in the liquid and the bubbles spread out. A careful examination of the bubble distribution shows that the bubbles in front and back move faster than the bubbles in the middle, leading to an asymmetric distribution of the bubbles. In the front, the fast moving bubbles race ahead, leaving the more crowded bubbles behind, but in the back the fast moving bubbles catch up with the bulk of the bubbles, increasing the local void fraction. Eventually (frame d) the bubbles have spread out sufficiently so that the local void fraction has been reduced essentially everywhere beyond its initial value.

In addition to the case shown in Fig. 3, we ran four other ones with similar, but slightly different, initial conditions. Although the detailed evolution of each case differed from the others, the overall evolution was

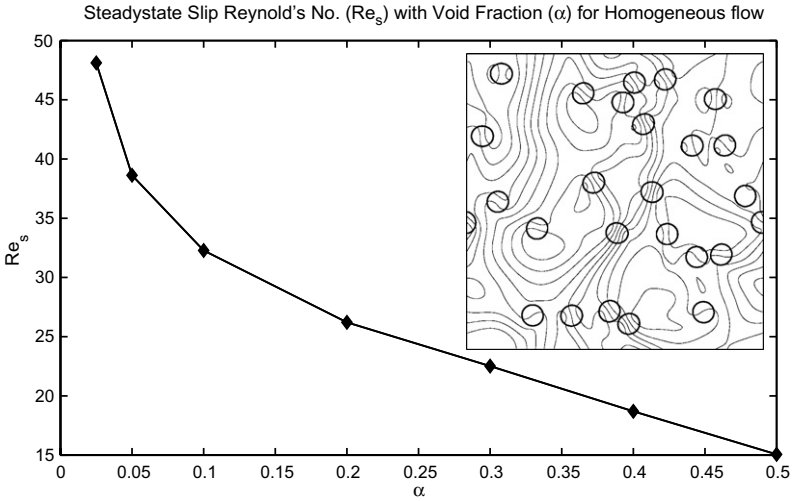

Fig. 2. The steady-state slip Reynolds number for bubbles in homogeneous flow versus the void fraction. The results are obtained by numerical simulations of the motion of 25 bubbles in a fully periodic domain. One frame, showing the bubble distribution at one time is inserted.

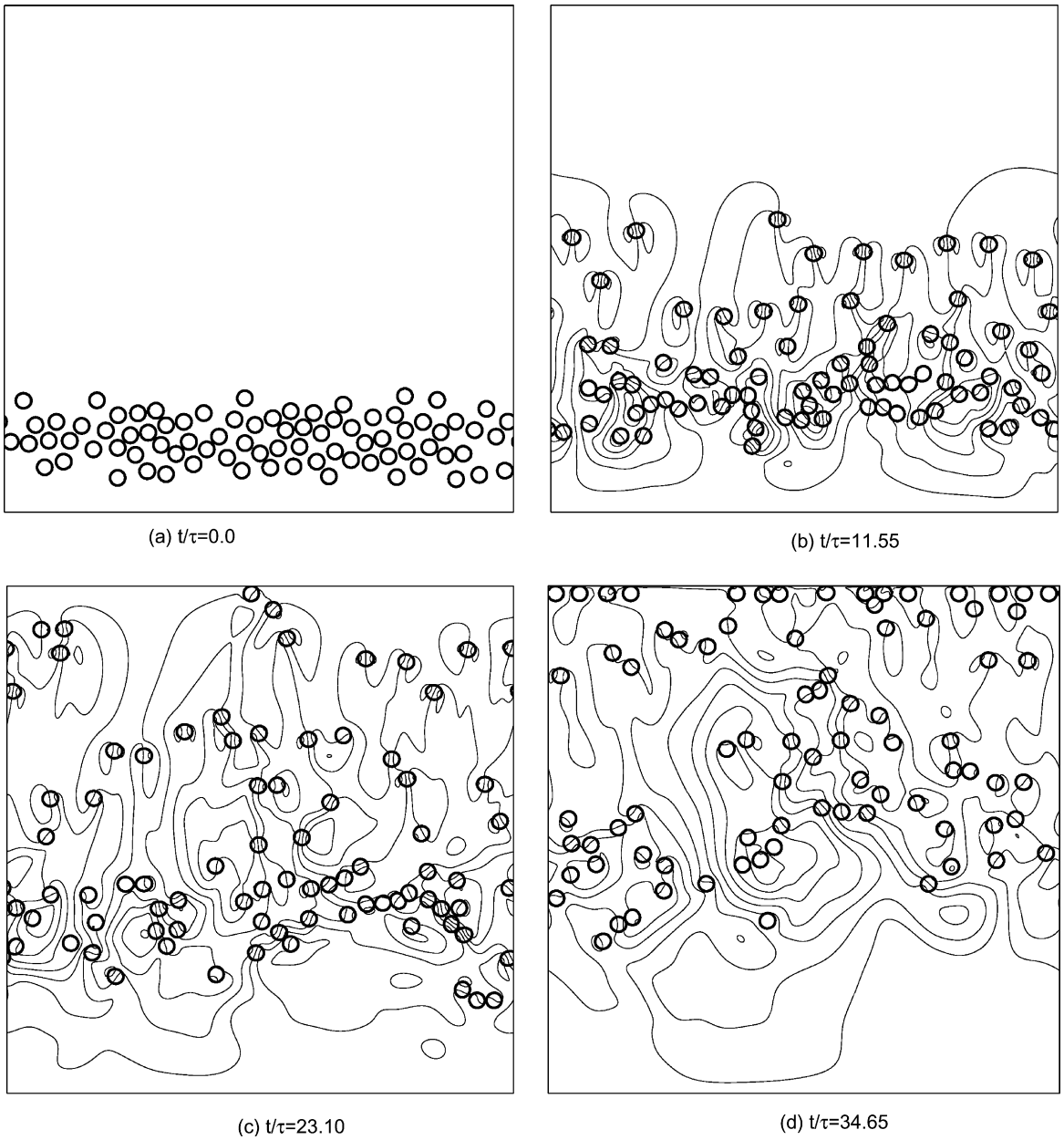

Fig. 3. Simulations of the rise of bubbles in a horizontal channel. The bubbles and the streamlines in a stationary frame of reference are shown at four different times, starting with the initial conditions. In the last frame, some of the bubbles have hit the top wall.

similar. In Fig. 4 we plot the average bubble rise velocity, versus non-dimensional time for the five realizations. All cases behave in the same way. The bubbles first accelerate rapidly, overshooting a little (as usually seen for simulations of a homogeneous distribution of bubbles in periodic domains, see Esmaeeli and Tryggvason, 1999). The average bubble velocity then increases gradually, as the average void fraction decreases, until at non-dimensional time 20 or so, when some of the bubbles have hit the top wall. The relatively rapid convergence of the results, when ensemble averaged over a number of run is consistent with the results of Esmaeeli and Tryggvason (1999), where a rapid convergence was found for homogeneous two-dimensional flows. Bunner and Tryggvason (2002) observed similar behavior for fully three-dimensional bubbly flows.

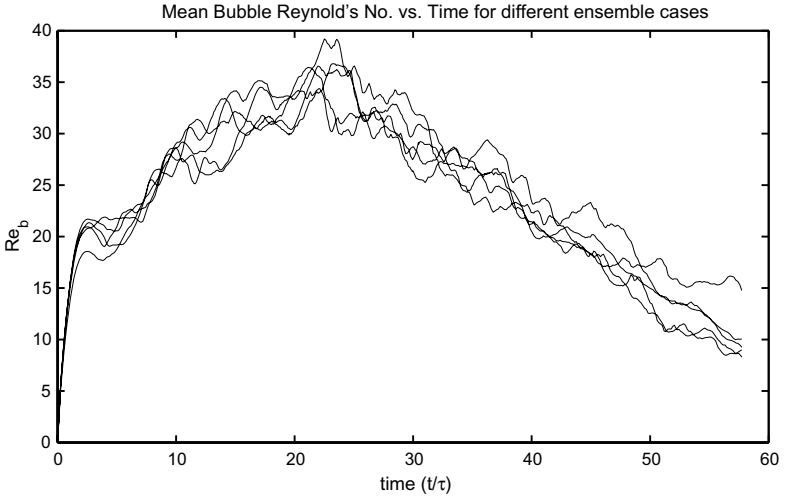

Fig. 4. The average bubble rise Reynolds number versus time for five different initial conditions. Initially the bubble velocity increases as the bubbles spread out and the void fraction decreases. After about time 20, some of the bubbles have hit the top wall and the average velocity decreases.

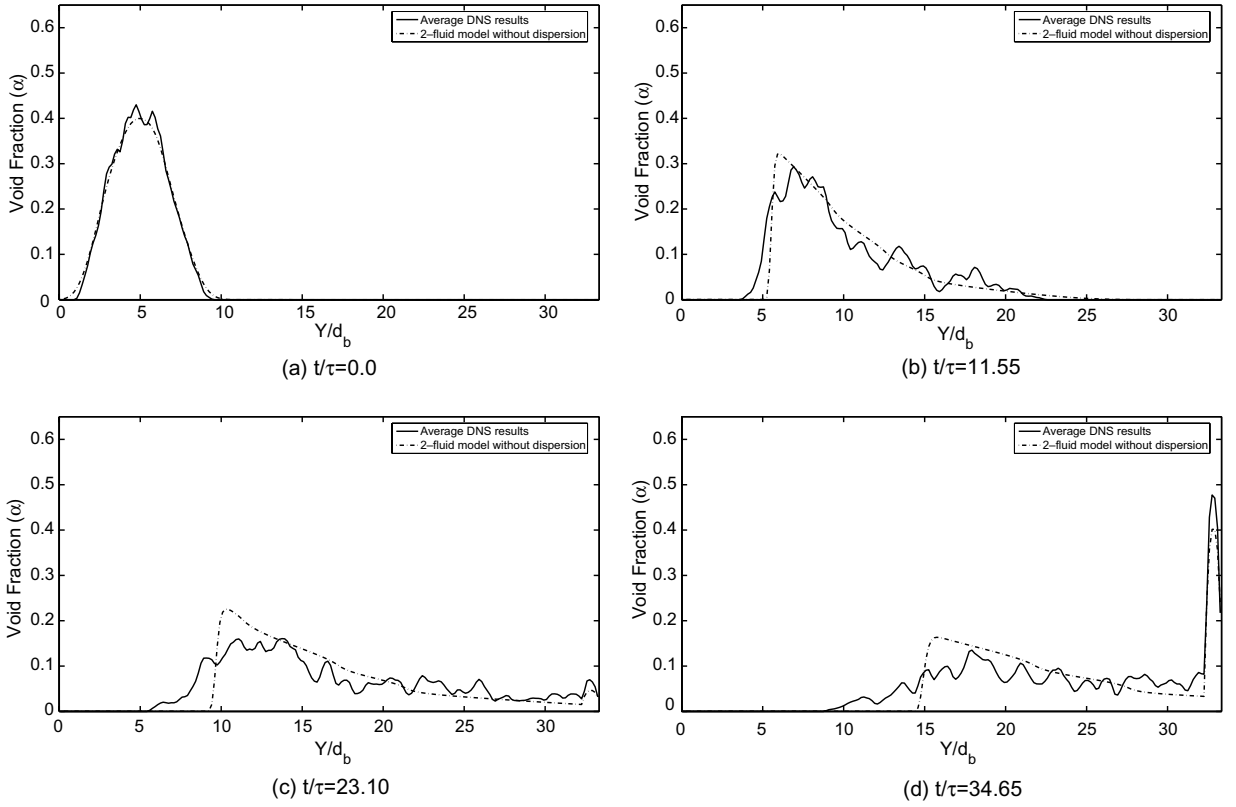

Fig. 5. The averaged void fraction profile at four different times. The solid line is the simulation results, averaged over five cases. The dashed line is the prediction of the two-fluid model.

In Fig. 5, we plot the void fraction profile obtained by averaging the result from five simulations (solid line) and those from the two-fluid model. The results are shown at four times, starting with the initial conditions.

The model void fraction profile is then evolved solving Eq. (1). To solve the one dimensional advection equation for the void fraction, we discretize the domain using 501 grid points. This is more than enough to give fully converged results for the parameters examined here. As initial conditions we use a smooth void fraction profile calculated from the ensemble average of the initial conditions for our numerical simulations. Since the slip velocity, v_s as a function of the void fraction, α, is already known, the time evolution of α is calculated by marching in time. To account for the gathering of bubbles at the top wall, we modify the model described by Eq. (1) in such a way that any void fraction flowing through a point one bubble diameter from the wall is simply allowed to accumulate at the wall. Since the velocity used to advect the void fraction profile increases with decreasing void fraction, the front part of the profile spreads out but the back side becomes steeper (frame b). The front side continues to spread (frames c and d), until the non-zero void fraction region hits the top wall where the bubbles accumulate (frame d). Although the results in Fig. 5 show that simply making the bubble slip velocity depend on the void fraction captures many aspect of the evolution reasonably well, it is also clear that some aspects are not modeled accurately. This is particularly true if we focus on the maximum void fraction and the shape of the profile in the back, where the increase in bubble velocity with the void fraction leads to a "shock." In the simulations the sharp change in the void fraction profile is smeared out and the maximum void fraction is reduced. Fig. 3, where the instantaneous streamlines are plotted, suggests that the reason for the difference is the absence of dispersion in the model. The rising bubbles stir up the liquid and the liquid velocity perturbs the motion of the bubbles. The simplest assumption is, therefore, that the dispersion of the bubbles is directly related to the turbulent kinetic energy.

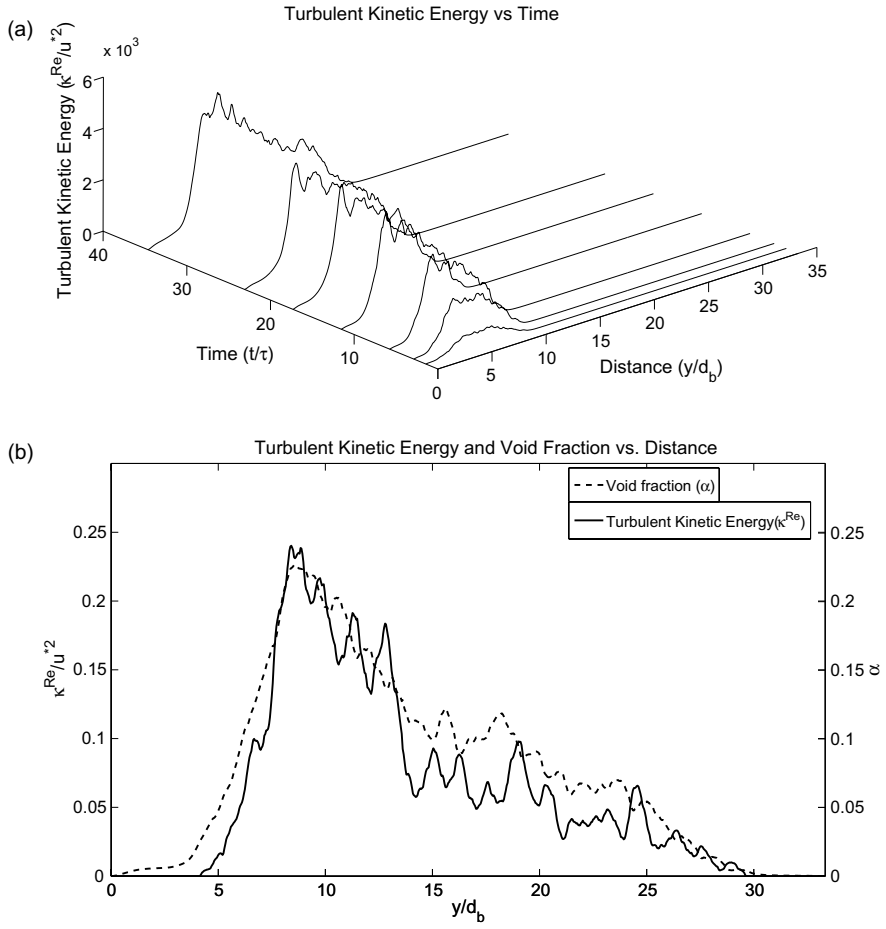

Fig. 6. (a) The average turbulent kinetic energy profile for one case, shown at seven times. (b) The void fraction and the turbulent kinetic energy versus y at $t/\tau = 34.65$.

To model the dispersion, we first have to examine the turbulent kinetic energy generated by the passage of the bubbles. In Fig. 6a we plot the averaged turbulent kinetic energy versus the vertical coordinate at different times. It is clear that the intensity of the turbulent kinetic energy increases over time and the stirred region both migrates upwards and spreads. To examine how closely the stirred region follows the location of the bubbles (as Fig. 2 suggests it does), we plot both the turbulent kinetic energy and the void fraction at a given time ($t/\tau = 3.0$) versus the vertical coordinate in Fig. 6b. Obviously, both profiles have a very similar shape.

To check if the turbulent kinetic energy and the void fraction always remain similar, we computed the correlation coefficient

$$r_{k\alpha} = \frac{\int_A (k - k_{av})(\alpha - \alpha_{av})\mathrm{d}y}{\sqrt{\int_A (k - k_{av})^2 \mathrm{d}y}\sqrt{\int_A (\alpha - \alpha_{av})^2 \mathrm{d}y}}$$

and in Fig. 7 we plot the correlation coefficient versus non-dimensional time for one particular simulation. Obviously, the kinetic energy and the void fraction profiles are very well correlated. Notice that both the kinetic energy and the void fraction profiles have been normalized by their average values. Thus, the correlation coefficient measures the similarities of their shapes at every given time, but says noting about how the relative magnitudes may change with time.

The bubble-induced kinetic energy in the liquid is often modeled by assuming that the flow around each bubble is a potential flow. This gives $k \sim \alpha v_s^2$ where v_s is the average slip velocity between the bubble and the liquid. Since v_s increases with decreasing void fraction, the total kinetic energy will increase as the bubbles disperse. This is easily seen as follows: If v_s is constant in a region of length Δ, then the total kinetic energy is $K_1 = \alpha v_s^2 \Delta$ (taking the proportionality coefficient to be unity). If the bubbles spread out over a length 2Δ, then the void fraction is $\alpha/2$. If the velocity increases by a factor of two (say), then the new total kinetic energy is $K_2 = (\alpha/2)(2v_s)^2(2\Delta) = 4K_1$. In Fig. 8, we plot the total kinetic energy, integrated over the whole domain, versus non-dimensional time. The kinetic energy increases with time, nearly linearly, until the bubbles start to accumulate at the top wall (around non-dimensional time 20). By comparing the total kinetic energy at two times, and using the results in Fig. 5 for the average void fraction and the size of the stirred zone, we see that the increase is not inconsistent with the estimate given above.

The diffusion coefficient also depends on the average size of the flow eddies in the stirred region in addition to the turbulent kinetic energy. In turbulence modeling the average dissipation is usually used to indicate the length scales of the velocity fluctuations and since a large eddy (small dissipation) is likely to move the bubbles

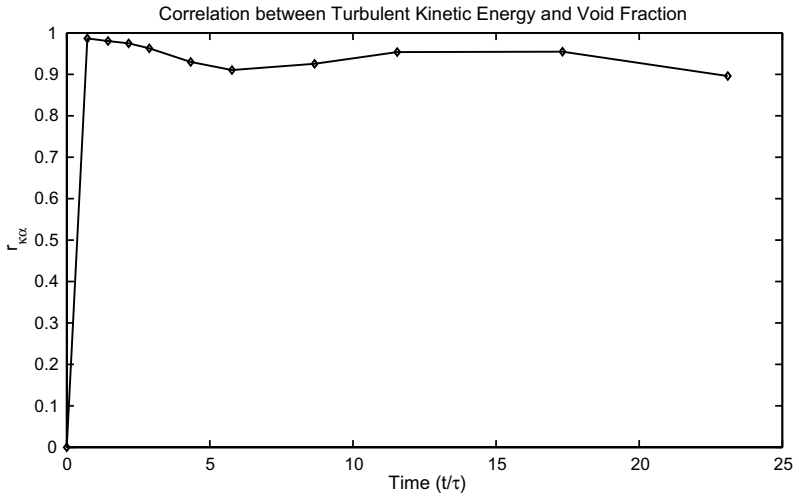

Fig. 7. The correlation coefficient (as defined in the text) between the turbulent kinetic energy and the void fraction versus time, for one case.

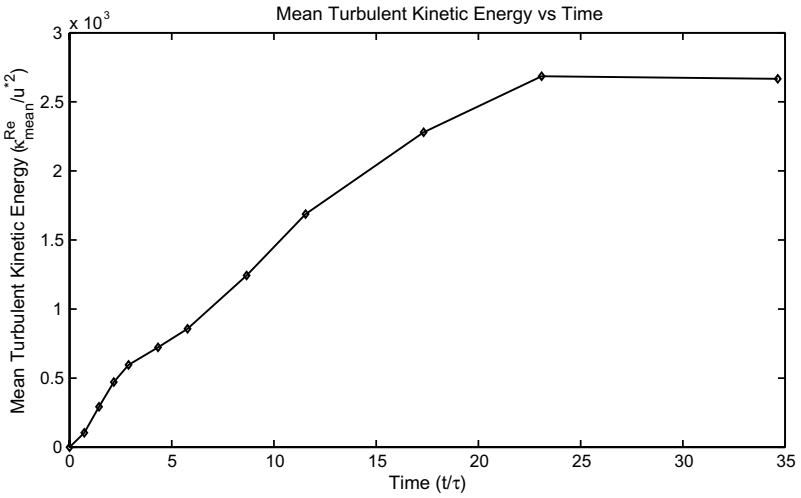

Fig. 8. The mean turbulent kinetic energy for one case versus time.

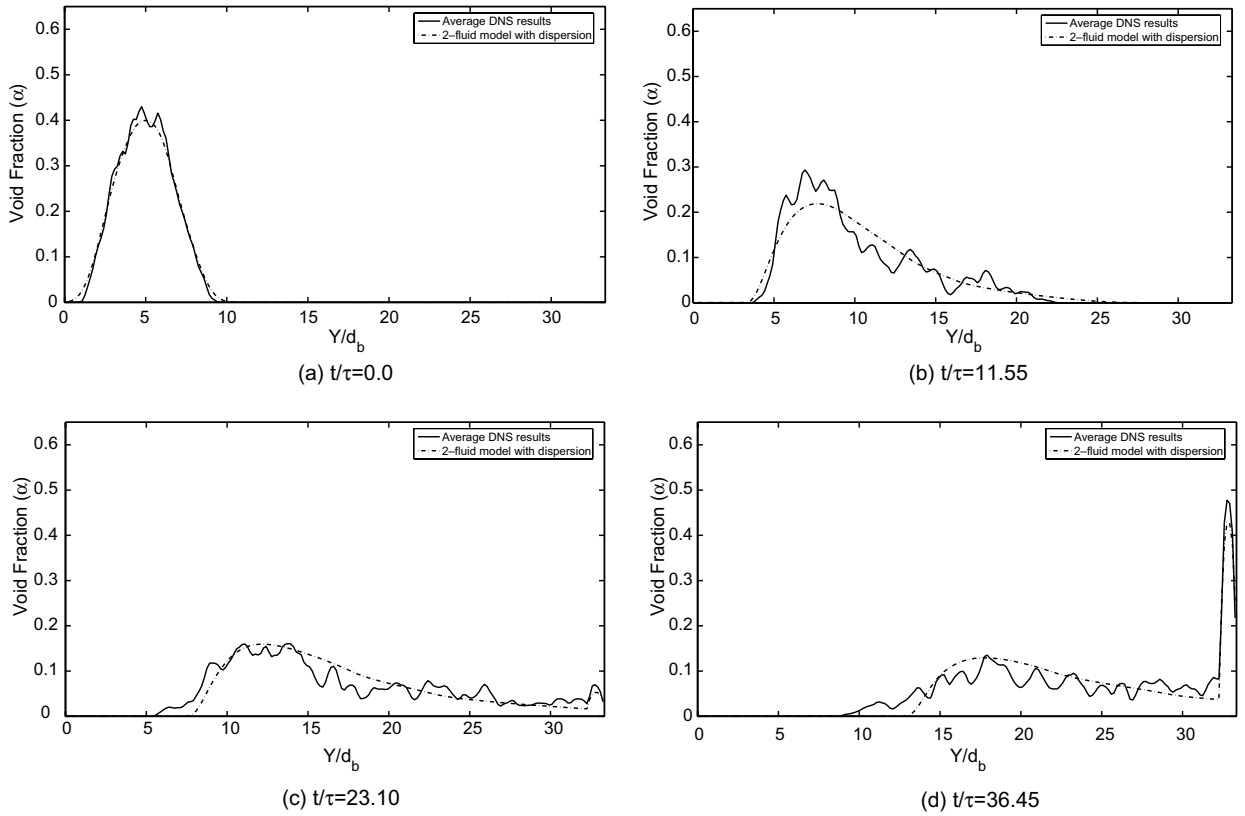

Fig. 9. The averaged void fraction profile from the simulations and as predicted by the two-fluid model at different times. Here $C\sqrt{d_b/g} = 2.0$ (see Eq. (6)).

more than a small eddy (high dissipation), the diffusion coefficient must be inversely proportional to the dissipation. On dimensional grounds, we have

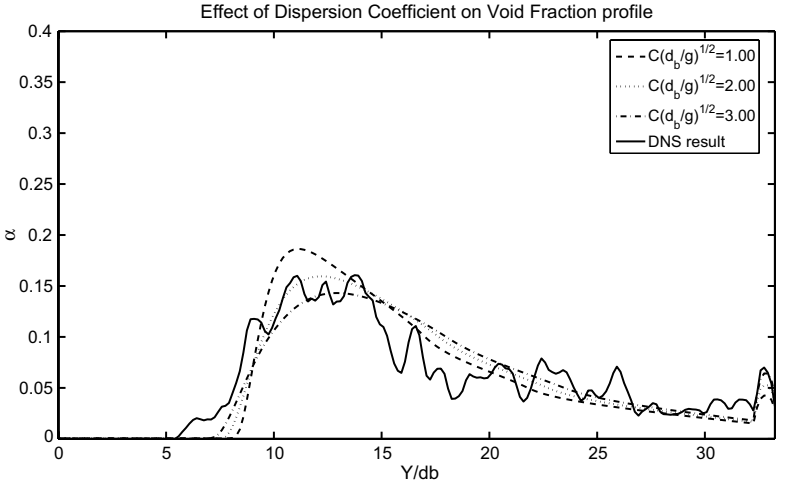

Fig. 10. The effect of the dispersion coefficient on the predicted void fraction profile at time $t/\tau = 46.20$. The average profile from the simulations is also plotted.

$$D \sim k^2/\varepsilon.$$

It seems reasonable to assume that the dissipation is proportional to the kinetic energy and a computation of the correlation coefficient between the dissipation and the kinetic energy shows that the correlation is comparable to the results for the kinetic energy and the void fraction, shown in Fig. 7 (Biswas, 2007). The diffusion coefficient will therefore be proportional to the kinetic energy. With the addition of dispersion, our model becomes

$$\frac{\partial \alpha}{\partial t} + \frac{\partial}{\partial y}(\alpha v_g) = \frac{\partial}{\partial x}\left(D(\alpha, v_g)\frac{\partial \alpha}{\partial y}\right) \tag{5}$$

with

$$D = C\sqrt{d_b/g}\alpha v_s^2 = C\sqrt{d_b/g}\frac{\alpha v_g^2}{(1-\alpha)^2}. \tag{6}$$

Here, we have written the adjustable coefficient as $C\sqrt{d_b/g}$ where C is a non-dimensional constant. We have compared the void fraction profile predicted by the model to the simulated results, using several different values for the constant C. In Fig. 9, we plot the comparison for $C\sqrt{d_b/g} = 2.0$, at several different times, in the same way as in Fig. 3. Overall the agreement is much better, showing that even the relatively simple model proposed above captures well what is going on. Since the void fraction profile from the simulations is not smooth (even after averaging it over five different realizations), we have not attempted to find the absolutely best C. While the results obviously depend on C, we have found that once we are in the right range, changing C somewhat does not change the agreement in major ways. In Fig. 10, we show the void fraction at non-dimensional time 46.20, along with model results for $C\sqrt{d_b/g} = 1, 2,$ and 3. The main difference between the model and the DNS results is at the back end of the profile, where the model under-predicts the dispersion of the bubbles. This is likely to be a result of ignoring the unsteady fluid motion behind the bubbles. As Fig. 3 shows, there is some unsteady residual motion left below the bubbles but the model relates the fluid turbulence directly to the non-zero void fraction. In addition to the results shown here, we have also done simulations of the bubble motion in larger domains (larger H) and find that the bubble motion is very similar to what has been presented here, up to the time when the bubbles hit the upper boundary.

4. Conclusions

Although the simulations presented here have been confined to two-dimensional systems, we have been able to show that data obtained from homogeneous systems can be used in more complex situations, at least as a

first approximation. The inclusion of a void fraction dependent rise velocity in the void fraction advection equation was sufficient to capture the spreading out of the bubbles in the front (where the void fraction is decreasing in the flow direction) and the clumping in the back (where void fraction is increasing). The simulations did, however, also show that the dispersion of the bubbles due to the unsteady flow generated by the bubbles must be included. Here we took a phenomenological approach and assumed a gradient type dispersion, directly linked to the pseudo-turbulence induced by the bubble motion. The data showed that the pseudo-turbulence distribution is well correlated with the void fraction distribution and we could therefore related the dispersion to the void fraction. This did, however, require an adjustable constant that is unlikely to be universal and the exact dependency of the dispersion on the void fraction distribution and the physical properties of the system (the Morton and Eotvos numbers) remains a topic for future investigation. The results showed that the kinetic energy of the liquid was well predicted by the void fraction distribution, suggesting that traditional modeling assumptions for the pseudo-turbulence hold reasonably well, at least for the parameters used here. Assuming a simple gradient diffusion model for the void fraction, with a diffusion coefficient proportional to the kinetic energy, allowed us to bring the model results and the DNS results into reasonable agreement.

Acknowledgement

This study was funded by the Department of Energy, Grant DE-FG02-03ER46083.

References

Antal, S.P., Lahey Jr., R.T., Flaherty, J.E., 1991. Analysis of phase distribution in fully developed laminar bubbly two-phase flow. Int. J. Multiphase Flow 17, 635–652.

Azpitarte, O.E., Buscaglia, G.C., 2003. Analytical and numerical evaluation of two-fluid model solutions for laminar fully developed bubbly two-phase flows. Chem. Eng. Sci. 58, 3765–3776.

Biswas, S., Esmaeeli, A., Tryggvason, G., 2005. Comparison of results from DNS of bubbly flows with a two-fluid model for two-dimensional laminar flows. Int. J. Multiphase Flow 31, 1036–1048.

Biswas, S., 2007. Direct numerical simulation and two-fluid modeling of multi-phase bubbly flows. PhD. Dissertation, Worcester Polytechnic Institute.

Bunner, B., Tryggvason, G., 2002a. Dynamics of homogeneous bubbly flows. Part 1. Rise velocity and microstructure of the bubbles. J. Fluid Mech. 466, 17–52.

Bunner, B., Tryggvason, G., 2002b. Dynamics of homogeneous bubbly flows. Part 2. Velocity fluctuations. J. Fluid Mech. 466, 53–84.

Bunner, B., Tryggvason, G., 2003. Effect of bubble deformation on the properties of bubbly flows. J. Fluid Mech. 495, 77–118.

Celik, I., Gel, A., 2002. A new approach in modeling phase distribution in fully developed bubbly pipe flow. Flow Turbul. Combust. 68, 289–311.

De Bertodano, M.L., Lahey Jr., R.T., Jones, O.C., 1987a. Phase distribution in bubbly two-phase flows in vertical ducts. Int. J. Multiphase Flow 13, 327–343.

De Bertodano, M.L., Lahey Jr., R.T., Jones, O.C., 1987b. Development of a k-ε model for bubbly two-phase flow. J. Fluids Eng. 13, 327–343.

De Bertodano, M.L., Lahey Jr., R.T., Jones, O.C., 1994. Phase distribution in bubbly two-phase flows in vertical ducts. Int. J. Multiphase Flow 20, 805–818.

Delhaye, J.M., Boure, J., 1982. General equations and two-phase flow modeling. J. Fluids Eng. 13, 327–343.

Drew, D.A., Passman, S.L., 1998. Theory of Multicomponent Fluids. Springer.

Esmaeeli, A., Tryggvason, G., 1996. An inverse energy cascade in two-dimensional, low Reynolds number bubbly flows. J. Fluid Mech. 314, 315–330.

Esmaeeli, A., Tryggvason, G., 1998. Direct numerical simulations of bubbly flows. Part 1. Low Reynolds number arrays. J. Fluid Mech. 377, 313–345.

Esmaeeli, A., Tryggvason, G., 1999. Direct numerical simulations of bubbly flows. Part II—Moderate Reynolds number arrays. J. Fluid Mech. 385, 325–358.

Esmaeeli, A., Tryggvason, G., 2005. A direct numerical simulation study of the buoyant rise of bubbles at O(100) Reynolds number. Phys. Fluids 17, 093303.

Guet, S., Ooms, G., Oliemans, R.V.A., 2005. Simplified two-fluid model for gas-lift efficiency predictions. AIChE J 51, 1885–1896.

Harlow, F.H., Amsden, A.A., 1975. Numerical calculation of multiphase flow. J. Comput. Phys. 17, 19–25.

Kataoka, I., Serizawa, A., 1989. Basic equations of turbulence in gas–liquid two-phase flow. Int. J. Multiphase Flow 15, 843–855.

Kuo, T.C., Pan, C., Chieng, C.C., Yang, A.S., 1997. Eulerian–Lagrangian computations on phase distribution of two-phase bubbly flows. Int. J. Numer Meth Fluids 30, 579–593.

Lu, J., Biswas, S., Tryggvason, G., 2006. A DNS study of laminar bubbly flows in a vertical channel. Int. J. Multiphase Flow 32, 643–660.

Politano, M.S., Carrica, P.M., Converti, J., 2003. A model for turbulent polydisperse two-phase flow in vertical channel. Int. J. Multiphase Flow 29, 1153–1182.

Prosperetti, A., Tryggvason, G. (Eds.), 2007. Computational Methods for Multiphase Flow. Cambridge University Press.

Spalting, D.B., 1980. Numerical computation of multi-phase fluid flow and heat transfer. In: Taylor, C., Morgan, K. (Eds.), Recent Advances in Numerical Methods in Fluid, vol. 1, pp. 139–167.

Tryggvason, G., Bunner, B., Esmaeeli, A., Juric, D., Al-Rawahi, N., Tauber, W., Han, J., Nas, S., Jan, Y.-J., 2001. A front tracking method for the computations of multiphase flows. J. Comput. Phys. 100, 25–37.

Unverdi, S.O., Tryggvason, G., 1992. A front tracking method for viscous incompressible flow. J. Comput. Phys. 169, 708–759.

Zhang, D.Z., Prosperetti, A., 1994. Averaged equations for inviscid disperse two-phase flow. J. Fluid Mech. 267, 185–219.